CFD BENCHMARK BASED ON EXPERIMENTS OF HELIUM DIPERSION IN A 1 M^3 ENCLOSURE - INTERCOMPARISONS FOR PLUMES

G. Bernard-Michel[1], B. Cariteau[1], J. Ni[2], S. Jallais[3], E. Vyazmina[3], D. Melideo[4], D. Baraldi[4] and A. Venetsanos[5]

[1] *D.E.N, D.A.N.S, S.E.M.T, L.T.M.F, Bât. 454, CEA Saclay, Gif-Sur-Yvette, France, e-mail : gilles.bernard-michel@cea.fr*
[2] *PSA Peugeot Citroën, Carrières-sous-Poissy, France, e-mail : jun.trochon@mpsa.com*
[3] *Air Liquide - Centre de Recherche Claude-Delorme, chemin de la Porte des Loges, Les loges-en-Josas 78354, France, e-mail : simon.jallais@airliquide.com*
[4] *Joint Research Center (JCR) European Commission, Institute for Energy and Transport, P.0. Box 2, 1755 ZG Petten, The Netherlands, e-mail : daniele.baraldi@jcr.nl*
[5] *National Centre for Scientific Reasearch Demokritos (NCSRD), Environnement Research Laboratory, 1530 Aghia Paraskevi, Attikis, Greece, e-mail: venets@ipta.demokritos.gr*

ABSTRACT

In the context of the French DIMITRHY project ANR-08-PANH006 experiments have been carried out to measure helium injections in a cubic 1 m^3 box - GAMELAN in a reproducible and quantitative manner. For the present work, we limit ourselves to the unique configuration of a closed box with a small hole at its base to prevent overpressure. This case leads to enough difficulties of modelisations to deserve our attention. The box is initially filled with air, and injections of helium through a tube of diameter 20 mm is operated. The box is instrumented with catharometres to measure the helium volume concentration within an accuracy better than 0.1%.

We present the CFD (Fluent and CASTEM, ANSYS-CFX and ADREA-HF) calculations results obtained by 5 different teams participating to the benchmark in the following situation: the case of a plume release of helium in a closed box (4NL/min). Parts of the CFD simulations were performed in the European co-funded project HyIndoor, others were performed in the french ANR-08-PANH006 DimitrHy project.

NOMENCLATURE

α	Helium concentration	μ	Viscosity [Pa.s]
μ_t	Turbulent viscosity [Pa.s]	ρ_{he}	Helium density [kg.m^{-3}]
ρ_a	Air density [kg.m^{-3}]	ρ	Mixture density [kg.m^{-3}]
σ	Schmidt number	C_s	Smagorinsky constant
d	Helium diffusivity to air [m^2.s^{-1}]	l_m	length of the convective jet [m]
Ri_0	Injection Richardson number	$\mathbf{g}$	Gravity acceleration vector [m.s^{-2}]
P	Pressure [Pa]	Q_{he}	Helium injection flow rate [m^3.s^{-1}]
$\mathbf{u}$	Mixture velocity [m.s^{-1}]	r	Radial coordinate [m]
r_i	Nozzle radius [m]	V_h	Cell surface [m^2]
z	vertical coordinate [m]		

I. INTRODUCTION

During the release of a buoyant fluid in an enclosure, its concentration builds up. When the buoyant fluid is a potentially flammable gas mixture, this built-up might endanger the safety of the persons or of the devices in the surroundings. As hydrogen is expected to come in widespread use in the near future, this problem of the concentration distribution in enclosures finds a renewed interest.

The distribution of the buoyant gas in the enclosure depends on many parameters, among them: the release rate, momentum and buoyancy flux, the volume of the enclosure and the position of the source. Different typical regimes have already been identified. We consider our enclosure as closed since the experimental results are studied in a time range where interactions with the decompression hole are negligible. Without ventilation, we find mainly two regimes depending on the ratio of the injected momentum to the potential energy required to mix the entire volume. If the injected momentum is high enough, the entire volume can be mixed resulting in a homogeneous concentration. If not, a vertical stratification takes place [1]. It is possible, for intermediate regimes, to find a homogeneous layer at the top of the enclosure, under which stratification takes place down to the bottom. If we have a closer look at the phenomenon, the jet or plume impacts the ceiling and spreads toward the side walls after that a horizontal density front moves downward. Baines and Tuner [2] give an analytical description of the velocity of the front and the final density profile once the front has reached the floor. Their model is extended by Worster and Hupper [3] to describe the time evolution of the vertical density profile during the first stage of the descending front. In some cases, Cleaver, Marshall and Linden [1] show that the vertical density profile exhibits a well-defined homogeneous layer near the ceiling under which the density varies linearly.

With these purposes, and more particularly in the scope of the project ANR PANH DIMITRHY, a set of experiments has been conducted in a small scale facility whose dimensions are typically those of a fuel cell, approximately 1 m^3 [4]. Helium was used as a model gas for hydrogen. For small injection momentum (less than 5 Nl/min), strong differences were observed between experiments and the model predicted concentrations [3] for a 5mm diameter nozzle and a 20mm diameter nozzle. Helium concentration profiles obtained with the 20mm nozzle are similar to those given

by the Worster and Hupper model [3], whereas concentrations measured with the 5mm nozzle are almost twice higher than predicted. Our goal was to explain those differences with the help of CFD calculations. The goal of this paper is to validate the CFD models through a benchmark, as a first step before the analysis of the faulty analytical models.

The present paper is organised as follows. The experimental techniques are presented in Section 2. Section 3 and 4 are devoted to the description of the numerical simulations: numerical scheme, mesh generation and turbulence model. Section 5 is dedicated to the comparisons between CFD calculations and experimental results. We conclude in section 6.

II. EXPERIMENTAL DESCRIPTION

We simulate an experimental set-up: a parallelepipic enclosure with a square base 0.93m wide and 1.26m high. One small vent of 10mm diameter is located 10mm from the floor in the middle of the back side. This vent is there to prevent the enclosure pressure to rise when the helium jet is released, see Figure 1. Helium concentrations are affected by the vent when - after a certain time - stratified or homogeneous layer reaches the bottom of the enclosure. This will be prevented by selecting a limited enough time range in our study.

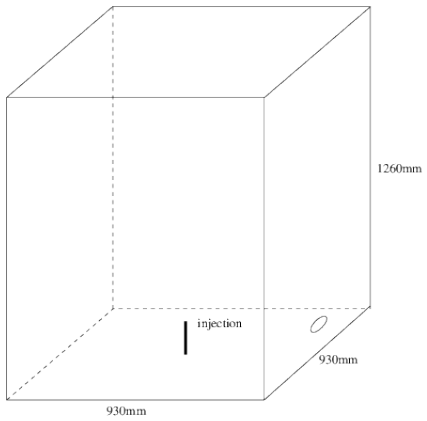

FIG. 1: Closed enclosure with a small aperture.

Local time variations of the volume fraction are measured by mini-catharometers TCG-3880 from Xensor. From manufacturer's information the long term absolute error on the volume fraction measurement is about 0.07%. The sensors are located at five levels along two vertical lines (see Fig. 2). The enclosure is placed in a garage with insulated walls. Temperature variations are lower than 0.1 °C.

Helium is injected either through a 20 mm diameter vertical nozzle whose exit is 210mm from the floor. The flow rate is controlled with mass flow regulators in between. We only focuse on results obtained for a flow rate of 4 Nl/min with a 20 mm diameter nozzle. A summary of the experimental conditions is given in Table I. With the diameter D of the nozzle, the density ρ_a of the ambient and ρ_{he} of the helium injected, the volumetric flow rate at the nozzle Q_{he} and the

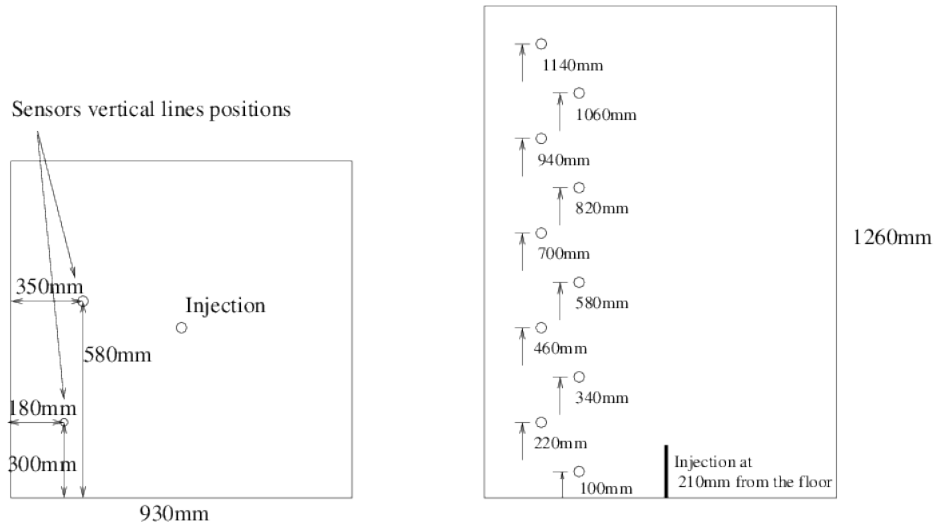

FIG. 2: Schematic representation of the experimental set-up with source and volume fraction measurement probes (cross) locations.

gravity acceleration g, the injection Richardson number is defined as (see e.g. [5]):

$$Ri_0 = \frac{\pi^2}{32}\frac{\rho_a - \rho_{he}}{\rho_{he}}\frac{gD^5}{Q_{he}^2} \tag{1}$$

Its order of magnitude for the selected flow rates is around 3, which indicates that the flow is slightly dominated by buoyancy as soon as the fluid exits the nozzle. We also introduce the average length of the jet at the injection nozzle, which indicates the transient distance ahead of which the jet becomes buoyant [6]: $l_m = 3Q_{he}/(S^{3/4}\sqrt{g'})$ where $g' = g(\rho_a - \rho_{he})/\rho_{he}$ is the reduced gravity and S is the injection surface of the nozzle. The length l_m varies from 0.03 m (for the 20 mm diameter nozzle) up to 0.3 m (for the 5 mm diameter), to be compared to the 1.26 m height of the enclosure.

TABLE I: Experimental conditions.

D (mm)	Q_{he} (Nl/min)	Ri_0	l_m (m)	T (°C)	injection time (s)
20	4	3	0.03	19.5	1200

III. VARIOUS MODELS AND CONSERVATION EQUATIONS

Common equations

We present here the equations common to all the participants.

a - Mixture mass conservation

$$\nabla.\mathbf{u} = 0, \tag{2}$$

where $\mathbf{u}$ is the mixture velocity.

b - Mixture momentum

$$\frac{\partial \rho \mathbf{u}}{\partial t} + \nabla . \rho \mathbf{u} \otimes \mathbf{u} = -\nabla P + \nabla \cdot ((\mu + \mu_t)\nabla \mathbf{u}) + \rho \mathbf{g}, \tag{3}$$

where P is the pressure of the mixture, μ, μ_t the laminar and the turbulent viscosity of the mixture and ρ the density of the mixture defined as $\rho = \alpha \rho_{he} + (1-\alpha)\rho_a$, where α is the volume fraction of helium in the mixture. We have taken $\mu = 1.9910^{-5}$kg/s for the laminar viscosity of the mixture.

The differences between the models considered by the participants are the following:

- AL, CEA and PSA uses a Boussinesq approximation for this equation.
- JCR uses an isothermal approach.
- NCSRD models the fully compressible equations.

c - Helium volume fraction

$$\frac{\partial \rho_{he} \alpha}{\partial t} + \nabla . \rho_{he} \mathbf{u} \alpha = \nabla . \left((\rho_{he} d + \frac{\mu_t}{\sigma}) \nabla \alpha \right), \tag{4}$$

The molecular diffusivity of helium to air is taken as $d = 5.649410^{-5}$ m/s as in [7], the turbulent Schmidt number $\sigma = 0.72$ and α is the helium volume concentration.

Different turbulent models used

a - Turbulent viscosity - L.E.S - CEA

$$\mu_t = C_s^2 V_h \sqrt{S_{ij} S_{ij}}, \tag{5}$$

Turbulence was modelled using a LES Smagorinsky model [8, 9] where $C_s = 0.2$ is the Smagorinsky constant, V_h is the surface of mesh where μ_t is evaluated, and S_{ij} the strain tensor.

b - K-ϵ and realizable K-ϵ turbulent model - AL, PSA, NCSRD, JCR We summarise the turbulent parameter in the table II.

TABLE II: k-ϵ parameters.

parameters	AL kϵ	AL realizable kϵ	PSA kϵ	NCSRD kϵ	JCR kϵ
Sc_t	0.7	0.7	0.7	0.85	0.7
C_μ	0.09	computed	0.09	0.09	0.09
$C_{1,\epsilon}$	1.44	1.44	1.44	1.44	1.44
σ_k	1	1	1	1	1
σ_ϵ	1.3	1.2	1.3	1.3	1.3
injection % turbulence	1%	1%	1%	?	5%

c - RNG k-ϵ turbulent model - NCSRD To be described.

d - SST turbulent model - JCR To be described.

Initial and boundary conditions

Initial conditions: temperature remains constant and equal to 292.5 K for the test case. Velocity and concentration are null at initial time.

Boundary conditions at the walls: the velocity is set to 0 at each wall of the enclosure. The normal derivative of the helium volume fraction α is set to 0, ensuring no diffusive flux of helium across the walls.

Small aperture for depressurisation: the concentration of helium is set to 0.

Injection nozzle: The way the injection flux of helium is set is described for each team, starting with the velocity:

- CEA - in the injection tube, 21cm before the injection surface, set a parabolic velocity profile matching the flow rate.
- AL - no precision (flux or velocity condition).
- PSA and JCR - constant velocity set to 0.227 m/s.
- NCSRD - fixed velocity, value estimated to preserve the flux on the none circular injection (4 cells).

For the helium volume concentration, the imposed conditions are the following:

- CEA - the volume concentration of helium is set to $\alpha = 1$, in the tube, 21 cm before the injection surface.
- AL, PSA, JCR and NCSRD - Helium concentration α set to 1 at the injection.

Symmetry plane: some teams used a symmetry plane in their approach. The boundary condition is a slipping condition for velocities and a null helium flux through the plan. CEA uses a 2D approach. On the axis, CEA imposes null fluxes, i.e. $\partial\alpha/\partial r = 0$ and $u_r = 0$.

Geometrical simplifications - CEA

Experimental results showed one-dimensional dependency of the helium volume concentration along the vertical axis [4]. Therefore it is not necessary to consider the original parallelepipic shape of the enclosure. CEA decided to simplify the geometry in their numerical simulations, as a first approach, considering a cylinder of the same height and the same section as the original enclosure, see Figure 3.

This geometry captures correctly the initial jet, which mainly occupies the centre of the enclosure. The concentration distribution being only dependent on the vertical position in the rest of the enclosure, the cross section's shape is not important if the area is conserved. CEA considers also the flow to be asymmetric around the jet injection axis. CEA knows from BOS visualisation of the concentration gradients in the experiments that the jet is not purely asymmetric [4], at least when it is purely buoyant, as in the present case.

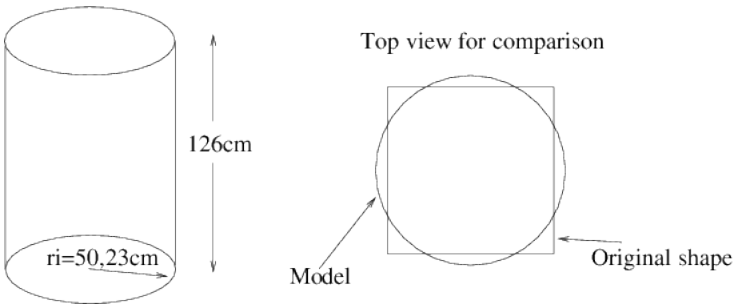

FIG. 3: Equivalent cylinder shape enclosure.

IV. GRID AND TIME DISCRETIZATION

We summarise for each team the main discretization parameters as well as the grids and time steps characteristics.

CEA

CEA uses the code **Cast3m** with quadratic 2D-axi finite elements for the velocity and the volume fraction discretization. CEA is using 3 nodes linear finite elements for the pressure. These elements satisfy the LBB conditions [10]. The scheme is implicit with an algebraic double projection method for the coupled mixture mass and momentum equations [11]. The convection scheme is centred.

The mesh is unstructured, composed of quadratic triangles. The strategy is to have a fine grid at the injection with at least 10 nodes on one injection radius, then along the axis, and at the top of the enclosure where a large vortex and 2 impacts with the top wall and the right wall are observed. The 2D mesh is made of 10000 nodes, the size of the cell is between 2 mm and 20 mm. The time variation discretization is an implicit BDF2 scheme [12]. The time step is $\delta t = 0.025\mathbf{s}$. Internal iterations for linearisation and for the projection method are performed to ensure a decrease of several oders of magnitude for the residual.

Air Liquide

The mesh is three-dimensional, exploiting the plan symetry of the geometry. Therefore only half of the domain is meshed. At least 8 nodes are placed along the injection diameter. The code used is Ansys Fluent. The mesh has approximately 500000 nodes. The time discretization is an implicit BDF2 scheme [12]. The time step is $\delta t = 0.001$s and is progressively increased up to 0.1s. Internal iterations for linearisation and for the projection method are limited to a maximum of 75.

PSA

The code used is Ansys Fluent. The mesh has 700,000 elements and exploits the symmetry of the problem. The time discretization is an implicit Euler scheme of order 1. Timesteps vary from 0.01 ms up to 0.1s with 50 internal iterations. The solver used is SIMPLE. The gradients are discretized with least square cell and the advective flux is discretized using an upwind scheme.

NCSRD

NCSRD uses the CFD code ADREA-HF [13]. A plane-symmetry is assumed (separate simulations without symmetry were performed and gave identical results). The geometry is meshed with a cartesian non-equidistant grid of 38x17x36 = 23,256 computational cells.

For the X-Grid: 2 cells of size 0.01m across the source, expanding away from it with expansion ratio 1.12. For the Y-Grid: a minimum cell size of 0.01m at the symmetry plane (Y=0), expanding away from it with expansion ratio 1.12. For the Z-Grid: a minimum cell size of 0.01m at the source, expanding away from it with expansion ratio 1.12.

The irregular geometry is handled using a porosity approach. NCSRD uses a 3rd order QUICK scheme for spatial discretization, and a first order fully implicit Euler scheme for temporal discretization. The time step is restricted by at a maximum CFL=2.

JCR

The mesh is assumed symmetrical. Different types of meshes have been analyzed (tetrahedral mesh with different refined zones). The selected one is the one with the finest discretization above the injection (at the top wall).

The CFD code used is ANSYS CFX 14.0. The advection scheme is "High Resolution". The transient simulation uses an imposed time step of 0.5 s. A simulation using an adaptive timestep scheme (starting with an initial time step of 0.001 s) shows similar results. The transient scheme is a second order backward Euler.

V. COMPARISONS BETWEEN NUMERICAL AND EXPERIMENTAL RESULTS

We compare the simulation results and the experimental results at the location of the 10 sensors, at 3 different timesteps, respectively 115s, 275s and 875**s** . We can observe, in Figures 4, 5 and 6, that experimental and numerical results show significant discrepancies.

At 115s (Fig. 4) we observe that the 3 laminar models, as well as CEA LES model, tend to overestimate the maximum concentration at the top of the box. It is understandable for the laminar approach which is less diffusive, not taking into account the existing turbulence (observed also on the experiments with BOS visualisation). The differences between the k-ε approaches are more surprising and it is possible that some of the participants encountered convergence issues due to not refined enough grids. The CEA approaches lead to higher maximum concentration, it is probably due to the 2D-axisymetry hypothesis but also to a much finer grid which strongly limitates numerical diffusion in laminar simulations.

At 275s (Fig. 5) the relative difference in the maximum concentration is diminishing compared to those observed at 115s. Otherwise, the remaining observed tendencies at 115s remain at 275s. We notice that the experimental results show the formation of an homogeneous layer at the top (between 0.9m and 1.2m), which is also found by the most diffusive k-ε approach (AL,JCR,PSA,NCSRD), although much thicker and for a concentration roughly 30% lower. Lam-

inar models and CEA LES do not show any homogeneous layer and but rather a more or less pronounced stratification. We note that laminar approach do not overestimate the experimental maximum concentration, except for CEA.

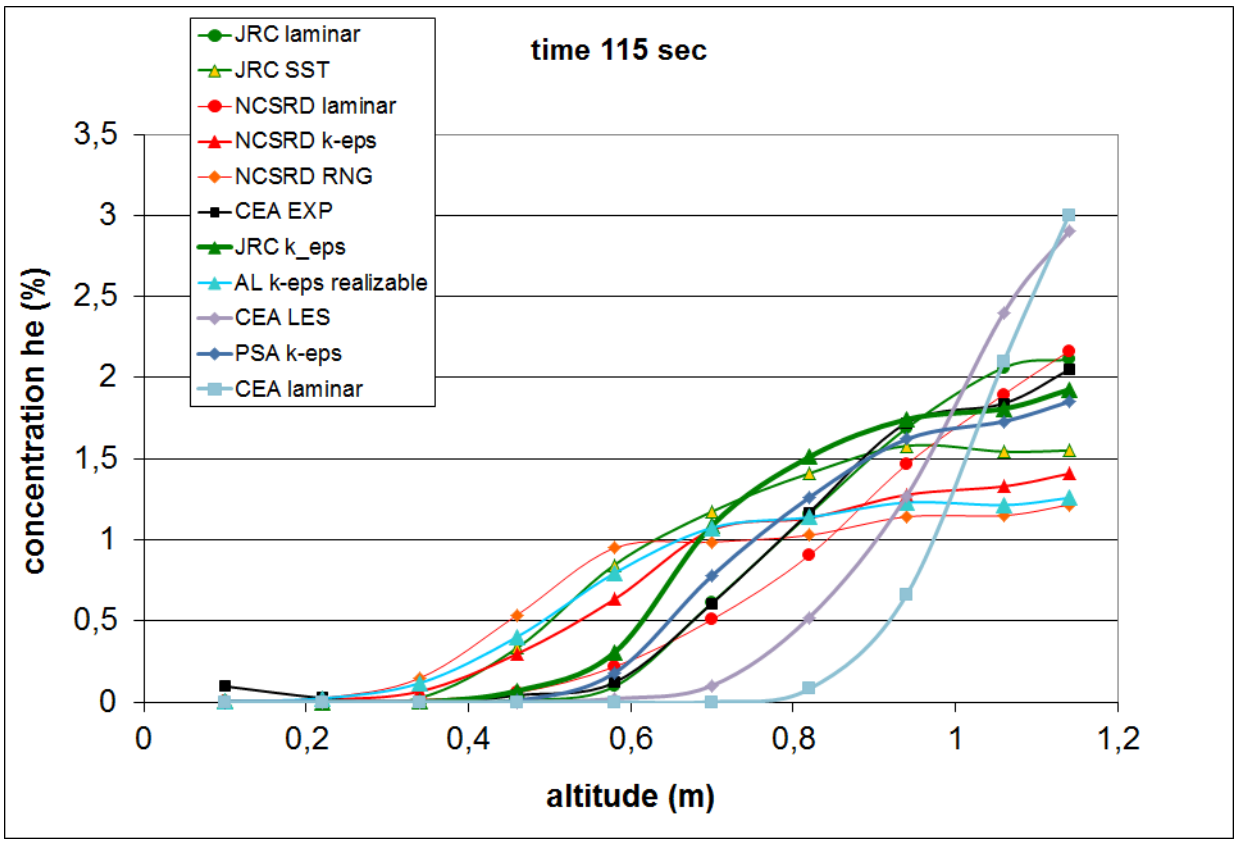

FIG. 4: Numerical versus experimental helium volume concentrations at the sensor locations with the 20mm nozzle - 115s.

At 875s (Fig. 6) the relative differences between maximum concentrations are even lower (approximately 25% of spreading). We notice nevertheless that the experimental measurements tend to be higher than all the CFD calculations, except at the very top sensor where CEA LES and laminar approaches show higher values of the maximum concentration. All the models reproduce the formation of a more or less homogeneous layer at the top, except for the CEA approaches.

We have roughly to types of results :

- the RANS turbulent approach, which gives more diffused results, with lower concentrations at the top and higher concentrations at the bottom of the box. This approach reproduces the formation of a homogeneous layer at the top but up to twice the size of the one found in the experiments. This approach is still too diffusive to be conservative.
- the laminar and LES approaches give similar results, with a tendency to overestimate the concentration (especially at lower times) at the top of the box due to an underestimated diffusivity. The formation of an homogeneous layer appears only at long times (875s) and its thickness is also overestimated. Those approaches are more conservative but can't be judged

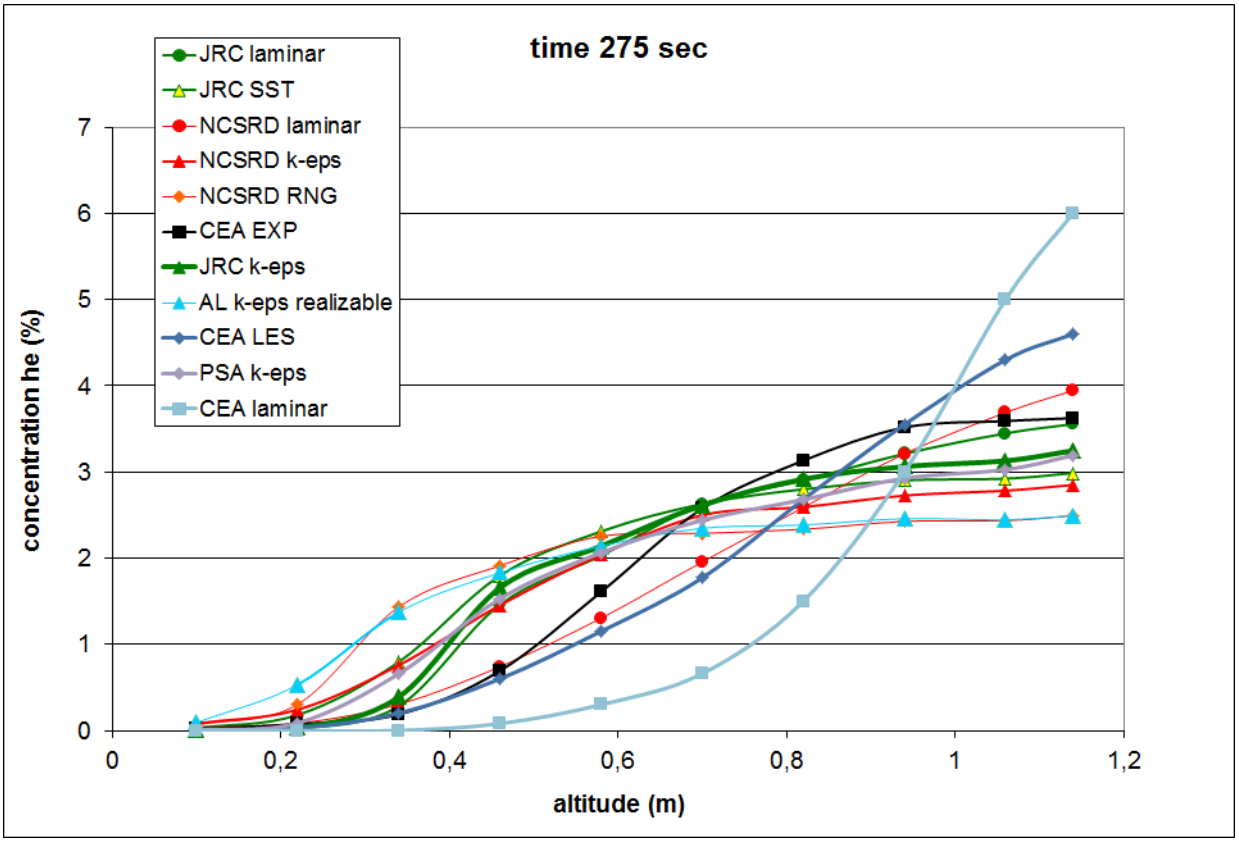

FIG. 5: Numerical versus experimental helium volume concentrations at the sensor locations with the 20mm nozzle - 275s.

to be more pertinent that k-ε. Indeed, the time increase of the maximum concentration is not well described.

- We also note that the experimental maximum concentration becomes higher than those of CFD calculations with increasing time. Indeed at 115s, 4 simulations show a maximum concentration higher than the experimental one, only 3 at 275s and only 2 at 875s. The rate of increase of the maximum concentration with time is higher in the experiments than in any of the simulations, with may be an exception for CEA laminar model.

VI. DISCUSSIONS AND CONCLUDING REMARKS

We have presented different numerical models to simulate an almost cubic enclosure for plume's injection of helium. The simulations produced overall good results, i.e. roughly less than 30% of discrepency compared to the experiments.

Nevertheless, the main characteristics of the helium distribution are not totally well reproduced:

- CEA approach leads to helium stratification, no formation of an homogeneous layer is ob-

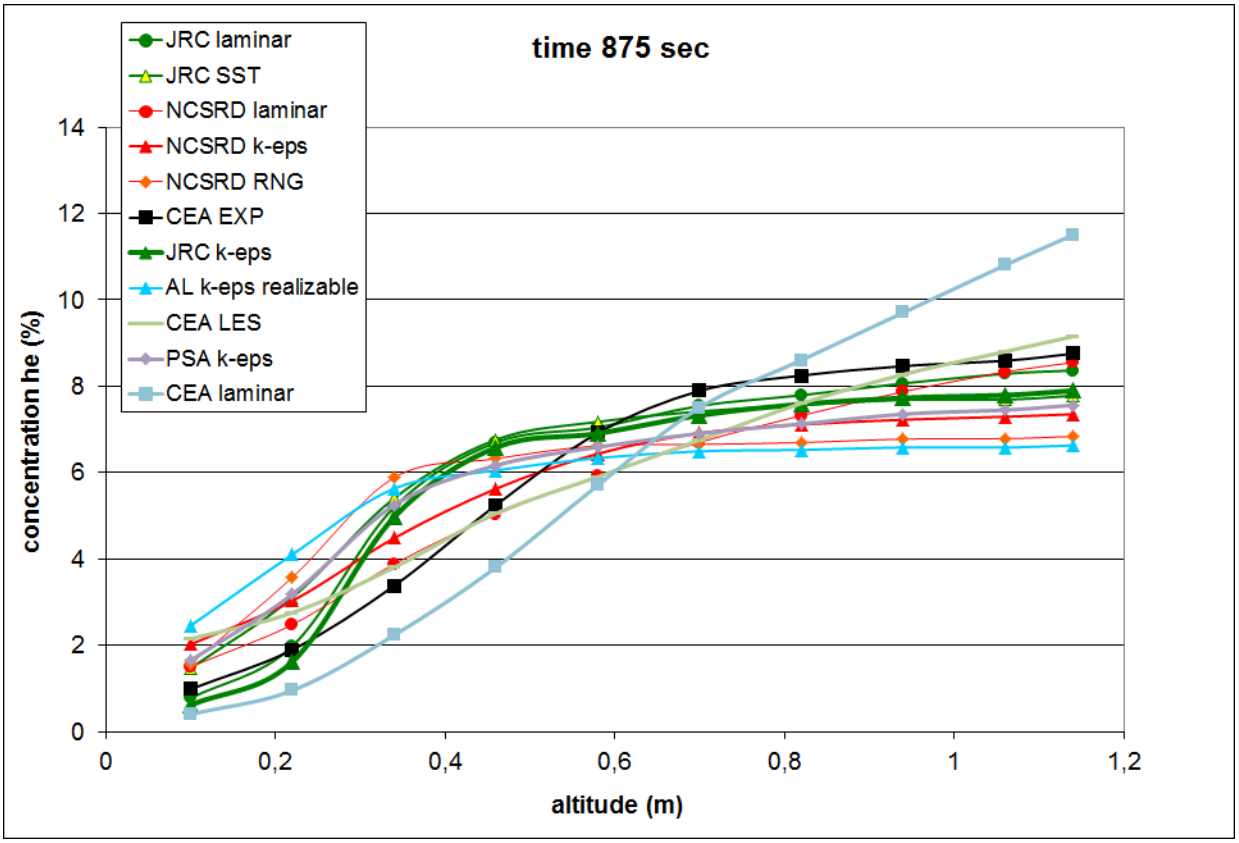

FIG. 6: Numerical versus experimental helium volume concentrations at the sensor locations with the 20mm nozzle - 285s.

served.

- AL, JRC, PSA and NCSRD k-ε approaches reproduce the formation of an homogeneous layer, yet approximately twice thicker and with lower concentrations, although JRC's results are slightly less diffusive (probably due to better grid convergence).

- laminar approach tends also to induce stratification, the apparition of an homogeneous layer starts only at long times (875s). If the maximum of concentrations are conservative, they progressively tend to be lower than those of the experiments when time increases. At long times, those simulations will also become too diffusive.

Our future objectives are to establish above which flow rate's threshold the k-ε approach gives accurate results. We will try also to understand the differences of results observed within the different k-ε approaches, especially in term of grid convergence. It is also planned to rerun the experiments with PIV measures in order to have access to velocity fields for improved comparisons with CFD.

VII. ACKNOWLEDGMENTS

This work was supported by the French Research National Agency (ANR) through the Plan d'Action National sur l'Hydrogène et les piles à combustible program (project DIMITRHY n°ANR -08-PANH-006) and by the HyIndoor project. The Hyindoor project is funded by the Fuel Cells and Hydrogen Joint Undertaking, a public-private partnership between the European Commission, fuel cell and hydrogen industries represented by the NEW Industry Grouping and the research community represented by the Research Grouping N.ERGHY.

---

[1] P. F. Linden, G. F. Lane-Serff, and D. A. Smeed, *Emptying filling boxes : the fluid mechanics of natural ventilation*, J. Fluid Mech. **212**, 309 (1990).
[2] W. D. Baines and J. S. Turner, *Turbulent buoyant convection from a source in a confined region*, J. Fluid Mech. **37**, 51 (1967).
[3] M. G. Worster and H. E. Huppert, *Time-dependant density profiles in a filling*, J. Fluid Mech. **132**, 457 (1983).
[4] B. Cariteau, Rapport DM2S/SFME/LEEF RT/2010-016/A, CEA (2010).
[5] R. P. Cleaver, M. R. Marshall, and P. F. Linden, *The build-up of concentration within a single enclosed volume following a release of natural gas*, J. Hazardous Mater. **36**, 209 (1984).
[6] P. N. Papanicolaou and E. J. List, *Investigation of round vertical turbulent buoyant jets*, J. Fluid Mech. **195**, 341 (1969).
[7] M. R. Swain, E. S. Grilliot, and M. Swain, *Experimental verification of a hydrogen risk assessment method*, Chemical Health and Safety pp. 28–32 (1999).
[8] J. Smagorinsky, *General circulation experiments with the primitive equations: 1. the basic experiments*, Mon. weather rv. **91(3)**, 99 (1963).
[9] Launder, *Turbulence*, Heat and Mass Transfer pp. 231–287 (1978).
[10] I. Babùska, *The finite element method with lagrangian multipliers*, Numer. Math. **20**, 179 (1973).
[11] S. Badia and R. Codina, *Algebraic pressure segregation methods for the incompressible navier-stokes equations*, Archives of Computational Methods in Engineering **15**, 343 (2007).
[12] A. Ern and J.-L. Guermond, *Éléments finis: théorie, applications, mise en œuvre* (Springer, 2002).
[13] B. J. Venetsanos A.G., Papanikolaou E., *The adrea-hf cfd code for consequence assessment of hydrogen applications*, Int. J. Hydrogen Energy **35**, 3908 (2010).
[14] S. V. Patankar, *Numerical heat transfer and fluid flow* (Hemisphere, 1980).